

LOCAL HELIOSEISMOLOGY OF NEAR-SURFACE FLOWS

D. C. Braun, A. C. Birch, and C. Lindsey

NorthWest Research Associates Inc., Colorado Research Associates Division, 3380 Mitchell Ln, Boulder, CO, 80301 USA, dbraun@cora.nwra.com, aaronb@cora.nwra.com, clindsey@cora.nwra.com

ABSTRACT

We present initial inferences about flows deduced from seismic holography in the near-surface layers (from 3 to 30 Mm deep). One of our first applications is understanding the variation with depth of the holographic flow signatures of supergranulation. Forward modeling based on the Born approximation indicates that the depth of detectable supergranular flows may be on the order of a few Mm. An analysis of near-surface flows over a solar rotation indicates that mature sunspots show supergranular sized outflows with peak velocities ~ 300 -500 m/s while almost all other types of magnetic regions show similarly compact inflows. Many active-region flows exhibit a distinct pattern in radial vorticity, consistent with a faster rotation rate near sunspots.

1. INTRODUCTION

We are beginning a multi-year project to understand the structure and dynamics of the solar interior, especially the variation of magnetic activity, from analyses of helioseismic data using phase-sensitive holography. The project will include analysis of data from the Michelson Doppler Imager (MDI) onboard *SOHO* and the Global Oscillation Network Group (GONG). Goals of this comprehensive project include understanding the nature of the supergranulation, monitoring subsurface variations in the meridional circulation, and understanding other subsurface flows and their relation to solar activity. Parallel theoretical efforts are underway to understand the forward and inverse modeling problems, and to compare and test the results against other seismic signatures, models and numerical simulations of artificial wave fields. Here we describe the application of phase-sensitive holography to MDI data to study near-surface flows observed during Carrington rotation CR1988. Our results are divided into two main sections: (1) forward modeling of the depth of the supergranular flows, and (2) characterization of

near-surface (0-3 Mm) flows over a whole rotation

Helioseismic holography computationally propagates the observed surface manifestations of sound waves (p -modes) into a solar model to estimate the amplitudes of the waves propagating into and out of a focus point at a chosen depth and position in the solar interior. These amplitudes, called the ingress and egress, are estimated by a convolution of the surface oscillation signal with appropriate Green's functions (Lindsey & Braun, 2000). In phase-sensitive holography we consider temporal correlations between the egress and ingress. The phase of the Fourier transform of this correlation is sensitive to perturbations at or near the focus, and is proportional to the variations in p -mode travel-times produced by these perturbations.

The method employed for flow diagnostics is based on the egresses and ingresses computed in the *lateral vantage* employing pupils spanning 4 quadrants extending in different directions (east, west, north and south) from the focus (Braun & Lindsey, 2003). The antisymmetric phase shift, the difference in the phase perturbation of waves traveling from one pupil to its opposite and the phase perturbation of waves traveling in the reverse direction, is sensitive to horizontal flows near the focus.

Forward and inverse-modeling efforts of these correlations signatures have been started, with some initial results for supergranulation shown in the next section.

2. THE SUPERGRANULATION

Our previous analysis of the variation of the antisymmetric phase signatures due to the supergranular flow with the focus depth has indicated an apparent anticorrelation of the flow pattern at a focus depth below 10 Mm with the near surface (3 Mm) pattern (Braun & Lindsey, 2003). It is tempting to interpret this result as a return-flow in supergranular

cells. However, this reversal is consistent with the increasing contribution in the pupils of the oppositely directed surface flows in the neighboring supergranule cells.

To explore this possibility, we have computed forward models of the antisymmetric phase signatures assuming simple cellular flows. In general, the sensitivity, \mathbf{K} , of the anti-symmetric phase $\delta\phi^A$ to a small flow $\mathbf{v}(\mathbf{x})$ satisfies

$$\delta\phi^A = \int_{\odot} d\mathbf{x} \mathbf{K}(\mathbf{x}) \cdot \mathbf{v}(\mathbf{x}). \quad (1)$$

The computation of the sensitivity functions is a straightforward generalization of the methods described by Gizon & Birch (2002). We use the normal-mode Greens functions, source model, and damping model described by Birch (2004). Fig. 1 shows a sample kernel, with a pupil as indicated, and optimized for a focal depth of 7 Mm.

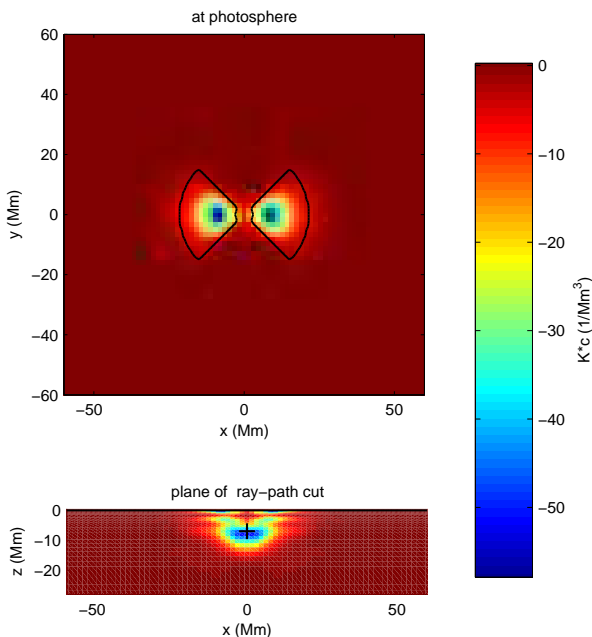


Figure 1. The x component of the kernel function as defined by Eq. 1, scaled by the local sound speed. The border of the pupil is shown in black. The panels show a horizontal slice at the photosphere (top), and a vertical slice at $y=0$.

The observed reversal in the flow signature below 10 Mm can be reproduced with a supergranule size of between 20 and 30 Mm, and the results are highly sensitive to the choice of the horizontal scale of the surface flow pattern (Fig. 2). We define the *velocity ratio* to be the ratio between the flow field at a given focus depth to the field at a focus of 3 Mm, as fit from a scatter plot (see Braun & Lindsey, 2003). The velocity ratio for a segment of the supergranule field observed with 28 hrs of MDI data is shown by the

blue line (after filtering to isolate flow components with wavenumbers between $80 < \ell < 200$). To model the observed variation with focus depth, we use a simple supergranule flow of the form

$$\mathbf{v}(x, y, z) = f(z)[\hat{\mathbf{x}} \sin(\pi x/L_s) \cos(\pi y/L_s) + \hat{\mathbf{y}} \cos(\pi x/L_s) \sin(\pi y/L_s)] \quad (2)$$

We neglect the vertical component of the flow. First, we assume an exponential decay with depth: $f(z) = e^{-z/z_0}$. The top panel in Fig. 2 shows that the reversal in the data can be reproduced with a horizontal length-scale parameter L_s on the order of 20-30 Mm, even with flows that are predominantly superficial ($z_0 = 0.1$ Mm). The bottom panel shows that a better fit to the data is obtained with a value of $z_0 = 2.5$ Mm. However, even with this deeper flow, it is apparent that the results are quite insensitive to the presence of a real supergranule turn-over. Here we have assumed $f(z) = e^{-z/z_0} \cos(\pi z/z_1)$, and the different symbols refer to different values of the parameter z_1 (“no return” corresponds to $z_1 \rightarrow \infty$). The different models shown in the bottom panel predict almost the same velocity ratios.

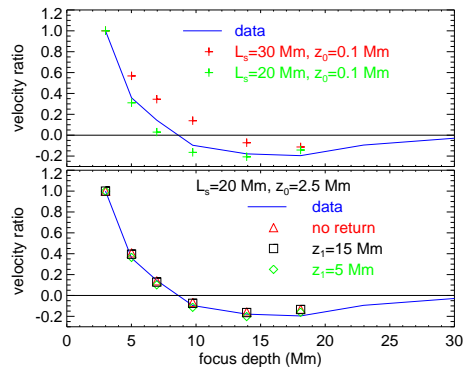


Figure 2. The variation of the supergranular velocity signatures with depth. The blue lines indicate the observations, while the symbols denote the results for several forward models (see text).

3. NEAR-SURFACE FLOWS AND ACTIVE REGIONS

To examine long-lived flows associated with active regions, we have computed near-surface flow signatures for the entire Carrington rotation CR1988 (2000 Mar 29-Apr 26). Here, we consider only a focal depth 3 Mm and assume that the flows do not vary significantly from 0-3 Mm. The horizontal components of the flow are in this case simply proportional to the antisymmetric phase signatures. A calibration constant is determined from tracking an area of the Sun at two different rates (e.g. the Carrington rotation rate, and the Carrington rate plus a fixed offset), and comparing maps of the phase differences for the two rates. For flows which actually vary with depth, the

inferred velocities deduced using this simple calibration may be considered as a (weighted) mean value from the surface to the focus depth, although caution should be exercised in this interpretation.

Almost all active regions are the sites of near-surface outflows or inflows. The flows (whether outflows or inflows) appear to be compact (roughly supergranular size, with peak velocities ~ 300 -500 m/s) and persist for most of the active region lifetimes. The middle panel of Fig. 4 shows the horizontal divergence of the flow pattern, averaged over 140 hours, and computed after the flows have been spatially smeared with a Gaussian with FWHM of 7.5° to reduce the supergranular contribution. In heliographic coordinates (L, B) , the horizontal divergence is given by

$$\nabla_{\mathbf{h}} \mathbf{v}_{\mathbf{h}} = (1/\cos B) [\partial(v_B \cos B)/\partial B + \partial v_L/\partial L], \quad (3)$$

where $\mathbf{v}_{\mathbf{h}} = (v_L, v_B)$. Several strong outflows (blue circles) and inflows (yellow circles) are identified in both the divergence maps and the magnetogram (top panel). A scatter plot of the divergence with magnetic flux density (middle panel of Fig. 3) shows the tendency for weaker active regions (e.g. without prominent sunspots) to show inflows and regions with spots to show outflows.

The radial component of the vorticity is shown in the bottom panel. First a “residual” flow $\mathbf{v}_{\mathbf{h}}^{\text{res}}$ is computed by subtracting a smooth function describing the surface differential rotation (Haber et al. (2002), table 1) from the zonal velocity component v_L . After smoothing, the radial component of the vorticity is computed from

$$(\nabla \times \mathbf{v}_{\mathbf{h}}^{\text{res}})_r = (1/\cos B) [\partial(v_B \cos B)/\partial L - \partial v_L/\partial B]. \quad (4)$$

A scatter plot of vorticity with flux density (Fig. 3, bottom panel) shows no clear trends in either hemisphere, but the vorticity map (Fig. 3, bottom panel) does indicate a tendency for sunspots (red contours) to occur near the boundaries of regions of opposite vorticity (typically positive to the north, and negative to the south). An examination of maps made of the two individual components (zonal shear and meridional shear) of the vorticity indicate this pattern is consistent with an excess in the rotation rate in magnetic regions. This excess rotation is directly visible in a scatter plot of the residual zonal velocity with magnetic flux density (upper panel in Fig. 3). Zhao et al. (2004) have noted a comparable rotational excess in weak magnetic fields. The top panel of Fig. 3 shows how this trend extends to larger magnetic flux densities typical of active regions and sunspots.

4. DISCUSSION

Our initial efforts to model the supergranulation have confirmed the suspicion (Braun & Lindsey,

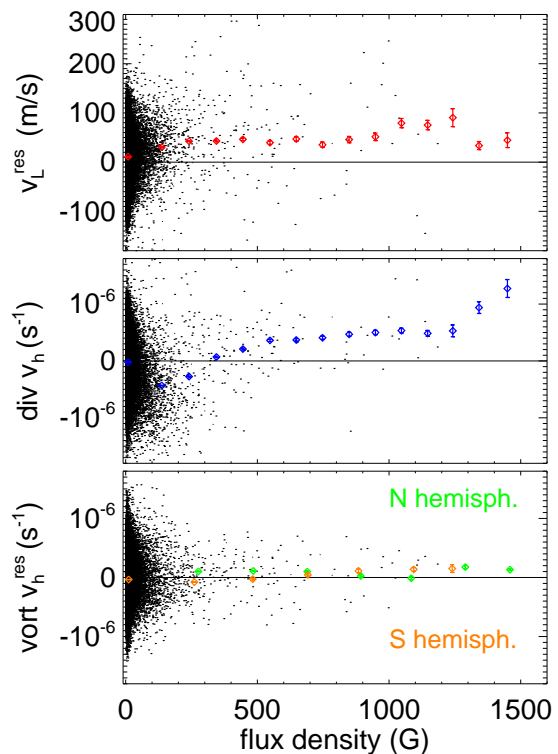


Figure 3. Scatter plots of the residual zonal velocity (top), the horizontal divergence (middle) and the radial vorticity (bottom) with magnetic flux density. The mean and standard-deviation of the mean are shown for bins of the flux density. For clarity, only a random subsample of the scattered points are shown. Because smoothing has been applied to the data, the standard-deviation of the mean probably underestimates the uncertainties.

2003) that the change in sign of the antisymmetric phase signatures below 10 Mm is the result of a predominantly surface contamination of the velocity signal from neighboring supergranules. We suspect that velocities from supergranulation may be highly peaked at the surface, and that the detection of a counter-flow may be a significant challenge. We intend to improve the models, by using the near-surface phase-signatures to constrain the horizontal structure, and to “focus” our attention to the near-surface (0-3 Mm depth) to improve these results.

Many techniques, based on both photospheric (e.g. Brickhouse & LaBonte, 1988) and helioseismic (e.g. Gizon, Duvall & Larsen, 2001; Haber et al., 2002; Zhao & Kosovichev, 2004) observations, have shown either inflows and outflows from sunspots and active regions. However, we are not aware of any previous determination of the clear trend of the divergence with the magnetic flux density as shown in the middle panel of Fig 3. A comparison of the expected line-of-sight component of the outflows around sunspots with integrated MDI Dopplergrams show that the

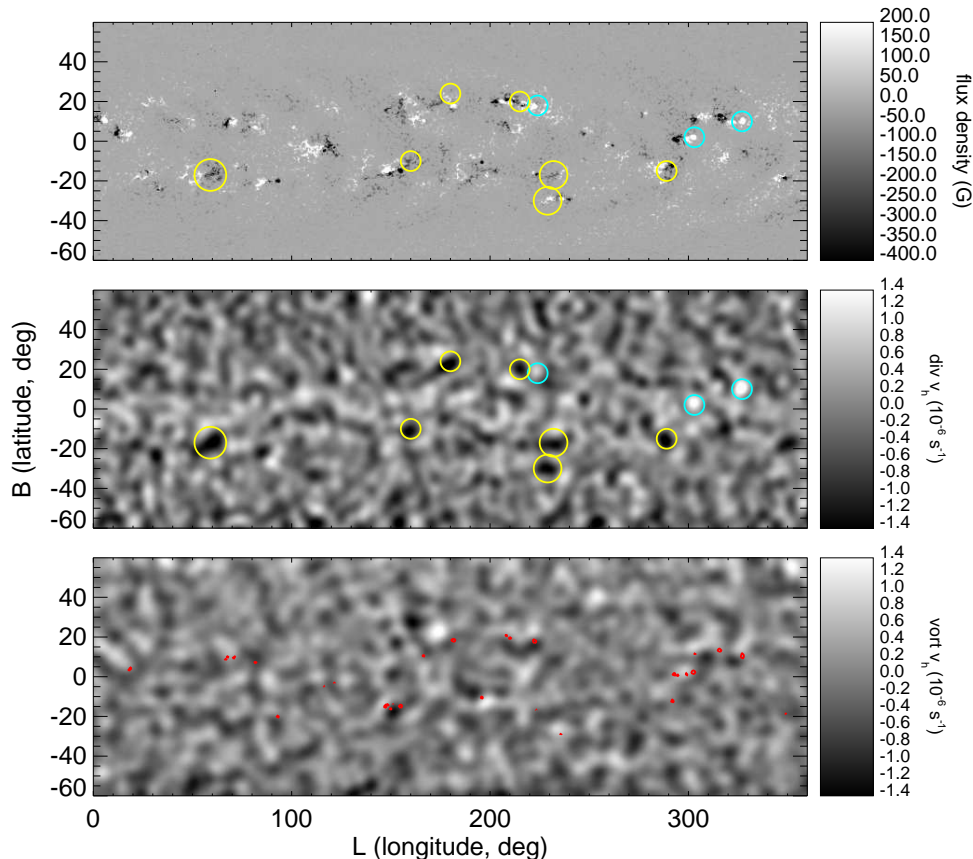


Figure 4. Top panel: A synoptic magnetogram for Carrington rotation 1988. Middle panel: The horizontal divergence of the near-surface flows. Blue (yellow) circles indicate a selected sample of outflows (inflows) which are also drawn over the magnetogram. Bottom panel: The radial component of the vorticity. Positive vorticity (white) indicates counter-clockwise motion, and negative (dark) vorticity has clockwise motion. Sunspots are indicated by red contours.

flows measured from holographic analysis in the top 3 Mm appear similar to, but a factor of two smaller in magnitude than, the photospheric flows. This suggests that the depth of these outflows may be less than 3 Mm, like the supergranulation. We intend to infer the depth variation of these flows, using forward and inverse modeling, and we will explore the possible artifacts that surface magnetic phase shifts and absorption may introduce in the results.

ACKNOWLEDGMENTS

This research is supported by the National Aeronautics and Space Administration through the Living With a Star and Sun-Earth Connection SR&T programs, and by the National Science Foundation through the Stellar Astronomy and Astrophysics program.

REFERENCES

- Birch, A.C., Kosovichev, A.G., and Duvall, T.L., Jr. 2004, *ApJ*, 608, 580
- Braun, D.C. and Lindsey, C. 2003, in *Local and Global Helioseismology: the Present and Future*, ed. H. Sawaya-Lacoste, ESA SP-517, (Noordwijk: ESA), 15
- Brickhouse, N.S. and LaBonte, B.J. 1988 *Sol. Phys.*, 115, 43
- Gizon, L. and Birch, A.C. 2002, *ApJ*, 571, 966
- Gizon, L., Duvall, T.L., Jr., and Larsen, R.M. 2001, in *Recent Insights into the Physics of the Sun and Heliosphere: IAU Symposium 203*, 189
- Haber, D., et al. 2002, *ApJ*, 570, 855
- Lindsey, C. and Braun, D.C. 2000, *Sol. Phys.*, 192, 307
- Zhao, J. and Kosovichev, A.G. 2004 *ApJ*, 603, 776
- Zhao, J., Kosovichev, A.G., and Duvall, T.L., Jr. 2004, *ApJ*, 607, L135